Design and Synthesis of Ruthenium Oligothienylacetylide Complexes. New Materials for Acoustically Induced Nonlinear Optics

Jean-Luc Fillaut,*,† Johann Perruchon,† Philippe Blanchard,‡ Jean Roncali,‡ Stéphane Golhen,⊥ Magali Allain,‡ Anna Migalsaka-Zalas,§ Ivan V. Kityk,∥ and Bouchta Sahraoui*,§

Institut de Chimie de Rennes, Organométalliques et Catalyse: Chimie et Electrochimie Moléculaires, CNRS UMR 6509, Université de Rennes 1, Campus de Beaulieu, 35042 Rennes Cedex, France, Laboratoire CIMMA, UMR CNRS 6200, Université d'Angers, 2 Boulevard Lavoisier, 49045 Angers Cedex, France, Laboratoire de Chimie du Solide et Inorganique Moléculaire, UMR 6511 CNRS, Institut de Chimie de Rennes, Université de Rennes 1, Campus Beaulieu 35042, Rennes Cedex, France, Laboratoire POMA, CNRS UMR 6136, Université d'Angers, 2 Boulevard Lavoisier, 49045 Angers Cedex, France, and Institute of Physics WSP, University of Czestochowa, Al. Armii Krajowej 13/15, PL-42217 Czestochowa, Poland

Received October 4, 2004

A series of new donor−π-acceptor ruthenium acetylide systems built around thiophene-based π-conjugating spacers of different lengths have been developed. Comparison of the linear and third-order nonlinear optical properties of these donor−π-acceptor chromophores shows that the elongation of the oligothiophene-based spacer or further introduction of a double bond leading to a dithienylethylene spacer produces a considerable bathochromic shift of the absorption maximum together with a dramatic enhancement of the molecular cubic hyperpolarizability. Furthermore acoustically induced second-harmonic generation (AISHG) has been observed for film composites of these complexes incorporated in PMMA matrixes and reaches values among the highest reported so far.

Introduction

Carbon-rich organometallics[1] containing rigid π-conjugated chains are important targets for the investigation of electron-transfer processes,[2] the formation of liquid crystalline materials,[1,3] and the construction of molecular devices[4] and novel materials for nonlinear optics (NLO).[5] Among them, σ-acetylide complexes represent one of the most widely investigated classes of second-order NLO metal complexes.[6] In these polarizable dipolar molecules, metal fragments are directly incorporated in the same plane as the π-conjugated pathway, which meets the requirements for the design of push−pull chromophores with large second-harmonic generation (SHG) efficiencies.[7] As for organic extended conjugated π-systems,[8] theoretical and experimental studies of σ-acetylide complexes have shown that large second-order hyperpolarizability (β) characterizing the molecular NLO efficiency depends on the strength of the donor, i.e., the metal, and acceptor groups and on the extent of the π-conjugated pathway. Moreover it has been suggested that the enhancement of metal−carbon multiple-bond character could enhance second-order nonlinear response.[9] Analogously to metallocenes, the metal acts as the donor group of the donor−π-acceptor structure and the second-order nonlinearity can be related to low-energy MLCT excitations. Noteworthy

* To whom correspondence should be addressed. E-mail: jean-luc.fillaut@univ-rennes1.fr. Fax: +33 223 23 69 39 (J.-L.F.). E-mail: bouchta.sahraoui@univ-angers.fr. Fax: +33 241 73 52 16 (B.S.).

† Institut de Chimie de Rennes, Université de Rennes 1

‡ Laboratoire CIMMA, Université d'Angers.

⊥ Laboratoire de Chimie du Solide et Inorganique Moléculaire, Université de Rennes 1.

§ Laboratoire POMA, Université d'Angers.

∥ University of Czestochowa.

(1) Long, N. J.; Williams, C. K. *Angew. Chem., Int. Ed.* **2003**, *42*, 2586.

(2) (a) Wong, K.-T.; Lehn, J.-M.; Peng, S.-M.; Lee, G.-H. *Chem. Commun.* **2000**, 2259. (b) Dembinski, R.; Bartik, T.; Bartik, B.; Jaeger, M.; Gladysz, J. A. *J. Am. Chem. Soc.* **2000**, *122*, 810. (c) Bruce, M. I.; Low, P. J.; Costuas, K.; Halet, J.-F.; Best, S. P.; Heath G. A. *J. Am. Chem. Soc.* **2000**, *122*, 1949.

(3) (a) Altmann, M.; Bunz, U. H. F. *Angew. Chem., Int. Ed. Engl.* **1995**, *34*, 569. (b) Oriol, L.; Serrano, J. L. *Adv. Mater.* **1995**, *7*, 348.

(4) (a) Lehn, J.-M. *Supramolecular Chemistry*: *Concepts and Perspectives*; VCH Publishers: Weinheim, Germany, 1995. (b) Ward, M. D. *Chem. Soc. Rev.* **1995**, *34*, 121. (c) Tour, J. M. *Acc. Chem. Res.* **2000**, *33*, 791.

(5) (a) Faust, R.; Diederich, F.; Gramlich, V.; Seiler, P. *Chem. Eur. J.* **1995**, *1*, 111. (b) Achar, S.; Puddephatt, R. *Angew. Chem., Int. Ed. Engl.* **1994**, *33*, 847. (c) Onitsuka, K.; Fujimoto, M.; Ohshiro, N.; Takahashi, S. *Angew. Chem., Int. Ed.* **1999**, *38*, 689. (d) Recent Developments in Metal Alkynyl Organometallic Chemistry. *J. Organomet. Chem.* **2003**, *670*.

(6) (a) Di Bella, S. *Chem. Soc. Rev.* **2001**, *30*, 355. (b) Whittall, I. R.; McDonagh, A. M.; Humphrey, M. G.; Samoc, M. *Adv. Organomet. Chem.* **1999**, *421*, 291. (c) McDonagh, A. M.; Humphrey, M. G.; Samoc, M.; Luther-Davies, B.; Houbrechts, S.; Wada, T.; Sasabe, H.; Persoons, A. *J. Am. Chem. Soc.* **1999**, *121*, 1405. (d) Powell, C. E.; Cifuentes, M. P.; Morrall, J. P.; Stranger, R.; Humphrey, M. G.; Samoc, M.; Luther-Davies, B.; Heath, G. A. *J. Am. Chem. Soc.* **2003**, *125*, 602.

(7) (a) Chemla, D. S.; Zyss, J. *Nonlinear Optical Properties of Organic Molecules and Crystals*; Academic Press: Orlando, FL, 1987. (b) Burland, D. M. *Chem. Rev.* **1994**, *94*, 1. (c) Marks, T. J.; Ratner, M. A. *Angew. Chem., Int. Ed. Engl.* **1995**, *34*, 155.

(8) (a) Marder, S. R.; Cheng, L.-T.; Tiemann, B. G.; Friedli, A. C.; Blanchard-Desce, M.; Perry, J. W.; Skindhøj, J. *Science* **1994**, *263*, 511. (b) Blanchard-Desce, M.; Alain, V.; Bedworth, P. V.; Marder, S. R.; Fort, A.; Runser, C.; Barzoukas, M.; Lebus, M. S.; Wortmann, R. *Chem. Eur. J.* **1997**, *3*, 1091.

(9) Calabrese, J. C.; Cheng, L.-T.; Green, J. C.; Marder, S. R.; Tam, W. *J. Am. Chem. Soc.* **1991**, *113*, 7227.

10.1021/om049236s CCC: $30.25
Publication on Web 01/13/2005

Scheme 1

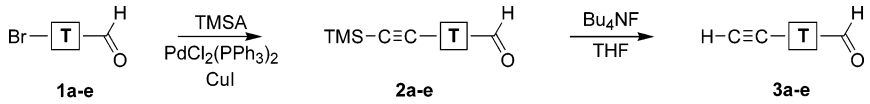

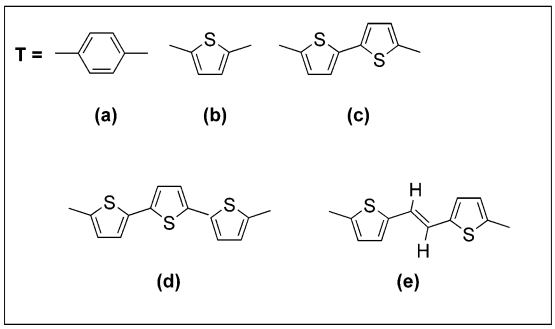

σ-acetylides, with an almost linear M−C≡C−R structure, give rise to a better coupling between the metal and the π-conjugated path and, hence, to larger optical nonlinearities. In this regard ruthenium(II) acetylide derivatives are among the most investigated alkynyl systems,[9,10] the ruthenium-alkynyl fragment being a powerful donor, which can compete with the strongest organic donors.[11]

Finally, recent studies identified these systems as powerful third-order NLO chromophores.[6c,12,13] These studies tend to indicate that it would be preferable to emphasize extended conjugated spacers rather than the strength of donor or acceptor groups of linear D−π-A structures.

In this work, we have studied the effect of π-bridge variation on cubic NLO properties of linear D−π-A ruthenium acetylide systems, using a constant donor−acceptor couple. These derivatives were constructed using a *trans*-[Cl−Ru(dppe)$_2$(−C≡C)] (dppe = diphenylphosphinoethane) unit linked to a formyl group, acting as the acceptor head, through various "π-conjugated spacer" units. Our interest focused on thiophene-based spacers such as oligothiophenes of various lengths and dithienylethylene. Indeed, thiophene oligomers can be regarded as one of the richest and more versatile systems for building organized structures across multiple length scales. In particular thiophene-based spacers are known to provide better effective conjugation than benzenoid moieties[14] and to lead to stable NLO chromophores with very high second-order hyperpolarizabilities.[15] These performances can be related to the moderate resonance energy of thiophene, which allows a better π-electron delocalization than, for example, benzene-containing spacers.[16] The results of electrochemical, linear optical, and cubic NLO measurements of the resulting ruthenium acetylide derivatives in solution will be described herein. We will also consider the use of these oligothienyl ruthenium derivatives as D−π-A chromophores in poled polymers.[17] Acoustically induced nonlinear optical properties[18] of these organometallic systems incorporated within polymethyl methacrylate (PMMA) matrixes will be presented.

Results and Discussion

Synthesis and Characterization of σ-Acetylide Complexes 4a−e. New acetylenes required for the syntheses of the alkynyl complexes **4a−e** were prepared by well-established organic synthetic procedures from their bromo precursors (Scheme 1).

These new acetylenes were characterized by IR, UV−vis, and NMR spectroscopy and mass spectrometry.

(10) Hurst, S.; Lucas, N. T.; Cifuentes, M. P.; Humphrey, M. G.; Samoc, M.; Luther-Davies, B.; Asselberghs, I.; Van Boxel, R.; Persoons, A. *J. Organomet. Chem.* **2001**, *633*, 114.

(11) (a) Lebreton, C.; Touchard, D.; Le Pichon, L.; Daridor, A.; Toupet, L.; Dixneuf, P. H. *Inorg. Chim. Acta* **1998**, *272*, 188. (b) Jayprakash, P. C.; Matsuoka, R. I.; Bhadbhade, M. M.; Puranik, V. G.; Das, P. K.; Nishihara, H.; Sarkar, A. *Organometallic*s **1999**, *18*, 3851.

(12) (a) Hurst, S. K.; Cifuentes, M. P.; Morrall, J. P. L.; Lucas, N. T.; Whittall, I. R.; Humphrey, M. G.; Asselberghs, I.; Persoons, A.; Samoc, M.; Luther-Davies, B.; Willis, A. C. *Organometallics* **2001**, *20*, 4664. (b) Hurst, S. K.; Cifuentes, M. P.; McDonagh, A. M.; Humphrey, M. G.; Samoc, M.; Luther-Davies, B.; Asselberghs, I.; Persoons, A. *J. Organomet. Chem.* **2002**, *642*, 259. (c) Hurst, S. K.; Humphrey, M. G.; Morrall, J. P.; Cifuentes, M. P.; Samoc, M.; Luther-Davies, B.; Heath, G. A.; Willis A. C. *J. Organomet. Chem.* **2003**, *670*, 56.

(13) Hurst, S. K.; Humphrey, M. G.; Isoshima, T.; Wostyn, K.; Asselberghs, I.; Clays, K.; Persoons, A.; Samoc, M.; Luther-Davies, B. *Organometallics* **2002**, *21*, 2024.

(14) (a) McCullough, R. D. *Adv. Mater.* **1998**, *10*, 93. (b) Roncali, J. *Chem. Rev.* **1997**, *97*, 173. (c) Kraft, A.; Grimsdale, A. C.; Holmes, A. B. *Angew. Chem., Int. Ed.* **1998**, *37*, 402. (d) Melucci, M.; Gazzano, M.; Barbarella, G.; Cavallini, M.; Biscarini, F.; Maccagnani, P.; Ostoja, P. *J. Am. Chem. Soc.* **2003**, *125*, 10266.

(15) (a) Raimundo, J.-M.; Blanchard, P.; Gallego-Planas, N.; Mercier, N.; Ledoux-Rak, I.; Hierle, R.; Roncali, J. *J. Org. Chem.* **2002**, *67*, 205. (b) Wu, X.; Wu, J.; Liu, Y.; Jen, A. K.-Y. *J. Am. Chem. Soc.* **1999**, *121*, 472. (e) Wu, X.; Wu, J.; Liu, Y.; Jen, A. K.-Y. *Chem. Commun.* **1999**, 2391. (c) Jen, A. K.-Y.; Liu, Y.; Zheng, L.; Liu, S.; Drost, K. J.; Zhang, Y.; Dalton, L. R. *Adv. Mater.* **1999**, *11*, 452−455. (d) Kim, O.-K.; Fort, A.; Barzoukas, M.; Blanchard-Desce, M.; Lehn, J.-M. *J. Mater. Chem.* **1999**, *9*, 2227 (e) Cai, C.; Liakatas, I.; Wong, M.-S.; Bösch, M.; Bosshard, C.; Günter, P.; Concilio, S.; Tirelli, N.; Suter, U. W. *Org. Lett.* **1999**, *1*, 1847. (f) Wu, I.-Y.; Lin, J. T.; Luo, J.; Li, C.-S.; Tsai, C.; Wen, Y. S.; Hsu, C.-C.; Yeh, F.-F.; Liou, S. *Organometallics* **1998**, *17*, 2188.

(16) (a) March, J. *Advanced Organic Chemistry*, 4th ed.; Wiley: New York, 1992; p 45. (b) Bird, C. W.; Cheeseman, G. W. H. In *Comprehensive Heterocyclic Chemistry*; Pergamon: Oxford, U.K., 1984; Vol. 4, pp 28−30. (c) Stott, Tracey L. Wolf, M. O. *Coord. Chem. Rev.* **2003**, *246*, 89.

(17) For general reviews on poled polymer NLO materials, see: (a) Marks, T. J.; Ratner, M. A. *Angew. Chem., Int. Ed. Engl.* **1995**, *34*, 155. (b) Burland, D. M.; Miller, R. D.; Walsh, C. A. *Chem. Rev.* **1994**, *94*, 31. (c) Bauer, S. *J. Appl. Phys.*: *Appl. Phys. Rev.* **1996**, *80*, 5531. (d) Khoo, I. C., Simoni, F., Umeton C., Eds. *Novel Optical Materials and Applications*; John Wiley and Sons: New York, 1997. (e) Bauer-Gogonea, S.; Gerhard-Multhaupt, R. In *Nonlinear Optical Polymers*; Gerhard-Multhaupt, R., Ed.; *Electrets*, 3rd ed.; 1999; Vol. II, pp 677−705.

(18) Nelson, D. F.; Lax, M. *Phys. Rev. B* **1971**, *3*, 2795.

Scheme 2

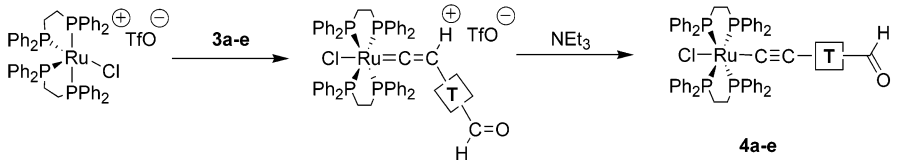

Table 1. Selected Bond Lengths (Å) and Bond Angles (deg) for 1e

bond lengths (Å)		bond angles (deg)	
Br−C(6)	1.871(8)	C(1)−C(2)−C(7)	128.7(7)
C(5)−C(6)	1.34(1)	C(2)−C(1)−C(3)	127.5(7)
C(4)−C(5)	1.40(1)	S(1)−C(3)−C(4)	108.9(6)
C(3)−C(4)	1.35(1)	S(1)−C(3)−C(1)	120.6(5)
C(1)−C(3)	1.43(1)	C(1)−C(3)−C(4)	130.5(7)
C(1)−C(2)	1.33(1)	S(2)−C(7)−C(2)	122.0(5)
C(2)−C(7)	1.42(1)	S(2)−C(7)−C(8)	109.4(6)
C(7)−C(8)	1.37(1)	C(2)−C(7)−C(8)	128.6(7)
C(8)−C(9)	1.38(1)	C(7)−S(2)−C(10)	91.1(4)
C(9)−C(10)	1.35(1)	S(2)−C(10)−C(9)	112.3(6)
C(10)−C(11)	1.52(1)	S(2)−C(10)−C(11)	120.7(5)
O−C(11)	1.08(1)	O−C(11)−C(10)	127.7(8)

(*E*)-1-(5-Bromo-2-thienyl)-2-(5-formyl-2-thienyl)ethene (**1e**) was prepared differently from the procedure described in the literature.[15f,19] Thus, selective bromination of formyldithienylethylene[15a] in the presence of *N*-bromosuccinimide in DMF readily afforded compound **1e** in 69% yield. Slow evaporation of a solution of **1e** in a mixture of dichloromethane and hexane gave crystals of good quality for X-ray determination. In the crystal, molecule **1e** adopts a fully planar conformation and the central carbon−carbon double bond shows an *E* configuration (Figure 1). Although these results concern the solid state, compound **1e** appears to be an excellent candidate for its use as π-conjugating spacer for NLO since it exhibits the entire requirement for an optimal electronic delocalization. Important bond lengths and angles are displayed in Table 1.

The synthetic methodologies employed for the preparation of the new ruthenium derivatives have been adapted from previously reported procedures.[20] The reaction of acetylenes **3a**−**e** and [*cis*-(Cl)($PPh_2CH_2CH_2PPh_2$)$_2$Ru][TfO][20b] in methylene chloride at room temperature for 20 h resulted in the formation of intermediate vinylidenes. Their complete formation was monitored by ^{31}P NMR spectroscopy. These vinylidenes were then cleaned by ether to remove the excess of free acetylene, before deprotonation with triethylamine (methylene chloride, room temperature, 1 h). The resulting alkynyl compounds were purified by a silica gel chromatography column (diethyl ether as eluent) and crystallized using a methylene chloride/hexane biphasic systems. Complexes **4a**−**e** were isolated as red crystalline powders in approximately 80% yields. All the spectroscopic data of compounds **4a**−**e** are consistent with their proposed structures. ^{31}P NMR spectra of all complexes contain one singlet resonance, consistent with the trans geometry at the ruthenium center. The chemical shifts of the C_α (141.5−154.5 ppm) and C_β carbons (106.8−115.8 ppm) of the (Ru−C_α≡C_β) in the ^{13}C NMR spectra are not significantly sensitive to changes in the acetylide ligands. However the larger upfield shift (154.5 ppm) of C_α in **4b** reveals that a slight contribution of a cumulenic form is perceptible in this complex that includes the shortest conjugated chain.[15f] The IR spectra of these complexes display a single characteristic ν(C≡C) absorption band (2040−2030 cm^{-1}) whose values are lower than those of the corresponding terminal or Me_3Si-substituted acetylide ligands as usually observed for acetylide ruthenium complexes.[20,21] The ^{1}H and ^{13}C NMR spectra of **4a**−**e** show features pertaining to the heteroaromatic and formyl groups: for instance, the *E* configuration of the central carbon−carbon double bond of the dithienylethylene fragment in **4e** is ascertained by a ^{1}H NMR doublet at 6.77 (1 H, $^3J_{HH}$ = 16 Hz) corresponding to one proton of the trans-CH=CH unit, the second H being masked by the phenyl groups of the dppe ligands. In each case, the respective molecular ion peaks [M]$^+$ were detected by electron impact mass spectroscopy.

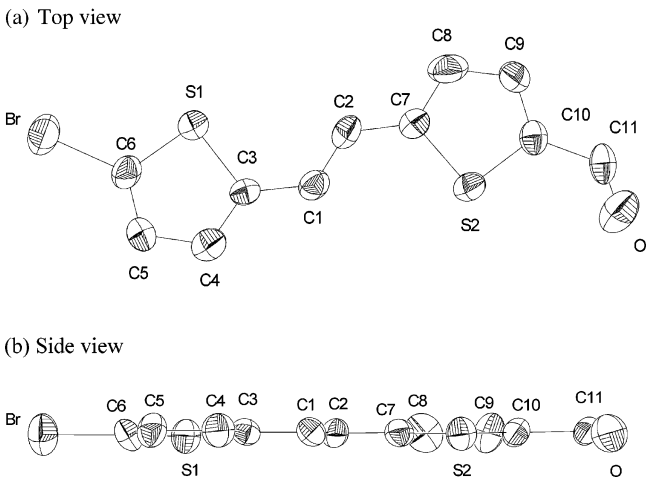

Figure 1. Top (a) and side (b) ORTEP views of **1e** showing 50% probability displacement ellipsoids and the atom numbering.

X-ray Structure of *trans*-[Ru(4-C≡C-th-CH=CH-th-CHO)(Cl)(dppe)$_2$], 4e. An X-ray diffraction analysis of **4e** (th = 2,5-substituted thiophene) confirmed the composition of this complex and especially the *E* configuration of the central double bond of the dithienylethylene fragment. The relevant bond lengths and angles for **4e** are displayed in Table 2. An ORTEP plot of **4e** with atom-labeling scheme is displayed in Figure 2.

The crystal structure consists of discrete dimeric molecules in which π-stacking between thiophene carboxaldehyde fragments of two molecules of **4e** results in a centrosymmetric packing (Figure 3), suggesting that no bulk second-order NLO responses would be observed.

(19) (a) Manecke, G.; Härtel, M. *Chem. Ber.* **1973**, *106*, 655. (b) Justin Thomas, K. R.; Lin, J. T.; Lin, K.-J. *Organometallics* **1999**, *18*, 5285.

(20) (a) Touchard, D.; Haquette, P.; Guesmi, S.; Pichon, L. L.; Daridor, A.; Toupet, L.; Dixneuf, P. H. *Organometallics* **1997**, *16*, 3640. (b) Touchard, D.; Dixneuf, P. H. *Coord. Chem. Rev.* **1998**, *178*−*180*, 409.

(21) Zhu, Y.; Millet, D. B.; Wolf, M. O.; Rettig, S. J. *Organometallics* **1999**, *18*, 1930.

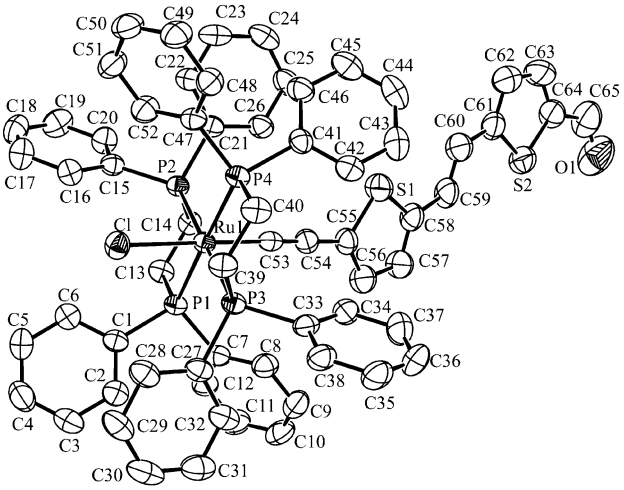

Figure 2. ORTEP drawing of **4e**, showing the atom numbering. Hydrogen atoms are omitted for clarity. Thermal ellipsoids are drawn at the 50% probability level.

Table 2. Selected Bond Lengths (Å) and Bond Angles (deg) for 4e

bond lengths (Å)		bond angles (deg)	
Ru(1)−P(1)	2.3641(10)	C(53)−Ru(1)−Cl	79.3(1)
Ru(1)−P(4)	2.3770(10)	C(54)−C(53)−Ru(1)	175.3(3)
Ru(1)−P(2)	2.3863(10)	C(53)−C(54)−C(55)	177.2(4)
Ru(1)−P(3)	2.3875(10)	C(56)−C(55)−C(54)	129.5(4)
Ru(1)−Cl	2.5099(10)	C(54)−C(55)−S(1)	121.3(3)
Ru(1)−C(53)	1.990(4)	C(56)−C(55)−S(1)	109.1(3)
C(53)−C(54)	1.197(5)	C(55)−C(56)−C(57)	113.5(5)
C(54)−C(55)	1.419(5)	C(58)−S(1)−C(55)	92.7(2)
C(55)−C(56)	1.380(6)	C(58)−C(57)−C(56)	114.4(4)
C(56)−C(57)	1.403(6)	C(57)−C(58)−S(1)	110.2(3)
C(57)−C(58)	1.349(7)	C(59)−C(58)−S(1)	122.7(4)
C(58)−C(59)	1.436(6)	C(57)−C(58)−C(59)	127.0(4)
C(59)−C(60)	1.326(7)	C(60)−C(59)−C(58)	129.1(5)
C(60)−C(61)	1.449(7)	C(59)−C(60)−C(61)	127.0(5)
C(61)−C(62)	1.372(8)	C(62)−C(61)−C(60)	129.3(5)
C(62)−C(63)	1.394(8)	C(60)−C(61)−S(2)	120.3(4)
C(63)−C(64)	1.374(8)	C(61)−C(62)−C(63)	113.3(5)
C(64)−C(65)	1.461(8)	C(64)−C(63)−C(62)	112.5(5)
O(1)−C(65)	1.216(8)	C(63)−C(64)−C(65)	126.7(6)
		C(62)−C(61)−S(2)	110.4(4)
		C(64)−S(2)−C(61)	91.9(3)
		C(63)−C(64)−S(2)	111.9(4)
		C(65)−C(64)−S(2)	121.4(5)
		O(1)−C(65)−C(64)	122.2(7)

Most bond lengths and angles about the Cl−Ru−C(53)−C(54)−C(55) units in this structure are classical. The Cl−Ru, Ru−C(53), and C(54)−C(55) data for this complex fall within the range of those previously reported for related octahedral *trans*-bis(bidentate phosphine)ruthenium alkynyl complexes.[12a,21,22] Of particular interest for NLO merit is the coplanarity of dithienylethylene units in the alkynyl ligand. Coplanarity, along with efficient delocalization, is important for maximizing NLO response in the present complexes.[23] The dihedral angle formed by the planes of the thienyl rings in **4e** (3.5(3)°) is close to coplanarity. It is interesting to compare this value with that in the precursor **1e**, in which the corresponding angle was evaluated to be 1.6°. The global structure of the dithienylethylene spacer is then almost conserved from **1e** to **4e**, with the thienyl rings being nearly coplanar, contributing to the extent of conjugation in the ruthenium complex **4e**.

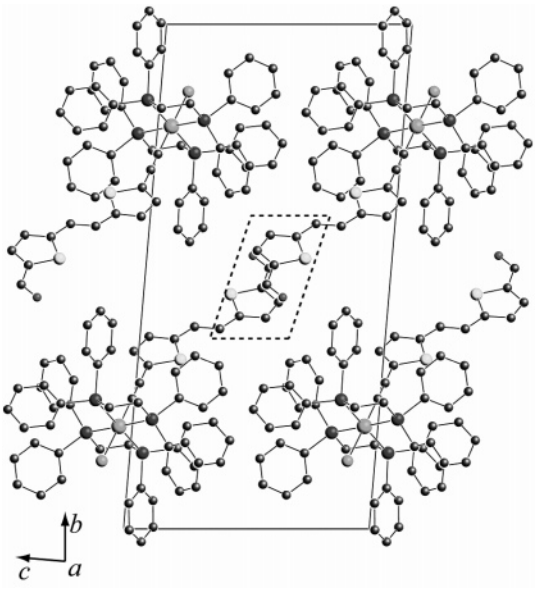

Figure 3. X-ray crystal structure of **4e**, showing the packing of individual molecules (dotted line).

Absorption Properties of Complexes 4. The electronic absorption spectra show broad bands with λ_{max} at 420, 450, 500, 510, and 530 nm for **4a**, **4b**, **4c**, **4d**, and **4e** (Table 3), which were attributed to MLCT transitions.[12a,24] Replacing the phenyl spacer as in **4a** by thienyl moieties in **4b**−**e** notably diminishes the HOMO−LUMO gap, due to an enhanced conjugation. Increasing conjugation in complexes **4b**−**d** through the introduction of more thienyl rings leads to an electronic transition of lower energy and an increase in the molar absorption coefficients. However, the extent of the induced red-shift decreases with increasing number of thienyl units. Thus, a red-shift of ca. 50 nm is observed from **4b** to **4c**, whereas the shift is only ca. 10 nm from **4c** to **4d**, corresponding to an increasing saturation of conjugation[25] in these complexes. However, the saturation of conjugation is less sensitive in the complex **4e**: a red-shift of ca. 30 nm is observed from **4c** to **4e** (to be compared to 10 nm from **4c** to **4d**). Replacing the terthiophene spacer as in **4d** by a dithienylethylene moiety significantly lowers the HOMO−LUMO gap.

Electrochemical Studies of Complexes 4. To get a deeper insight into the mutual donor−acceptor electronic influence from the ruthenium alkynyl moiety to the formyl end-group through the different spacers, we studied the redox properties of the complexes **4a**−**e** by cyclic voltammetry. The results are presented in Table 3. The compounds exhibit two reversible one-electron oxidation waves in their cyclic voltammograms in the range 0.0−1.8 V vs SCE. The first wave (ranging from 0.60 for **4a** to 0.39 V vs SCE for **4d**) was assigned to the metal-centered Ru(II/III) oxidation for all these compounds. The second wave can be attributed either to a Ru(III/IV) oxidation (**4a**) or to the oxidation of the thiophene-based spacers (**4b**−**e**). In **4a**, this wave at $E_{1/2}$

(22) Lebreton, C.; Touchard, D.; Le Pichon, L.; Daridor, A.; Toupet, L.; Dixneuf P. H. *Inorg. Chim. Acta* **1998**, *272*, 188.
(23) McDonagh, A. M.; Whittall, I. R.; Humphrey, M. G.; Skelton, B. W.; White, A. H. *J. Organomet. Chem.* **1996**, *519*, 229.
(24) Naulty, R. H.; McDonagh, A. M.; Whittall, I. R.; Cifuentes, M. P.; Humphrey, M. G.; Houbrechts, S.; Maes, J.; Persoons, A.; Heath, G. A.; Hockless, D. C. R. *J. Organomet. Chem.* **1998**, *563*, 137.
(25) Meier, H. *Chem. Eur. J.* **2004**, *10*, 360.

Table 3. Electronic Absorption and Cyclic Voltammetric Data for Complexes 4a−e

compound	λ_{max} (nm)[a] [ϵ (10^4 M^{-1} cm^{-1})]	$E_{1/2}$ (V)[b] [ΔE(mV)]	$E_{1/2}$ (V) [ΔE(mV)]
trans-[Ru(4-C≡CC_6H_4CHO)Cl(dppe)$_2$] (**4a**)	420 [1.3]	0.60 [80]	1.40[c] [100]
trans-[Ru(2,5-C≡CC-th-CHO)Cl(dppe)$_2$] (**4b**)	450 [2.7]	0.62 [80]	1.35[d] [100]
trans-[Ru(2,2′,5,5′-C≡C-th-th-CHO)Cl(dppe)$_2$] (**4c**)	500 [2.6]	0.46 [80]	1.20[d] [100]
trans-[Ru(2,2′,5,5′,2″,5″-C≡C-th-th-th-CHO)Cl(dppe)$_2$] (**4d**)	510 [3.2]	0.39 [80]	0.99[d] [100]
trans-[Ru(−C≡C-th-(*E*)CH=CH-th-CHO)Cl(dppe)$_2$] (**4e**)	530 [5.5]	0.41 [80]	1.06[d] [100]

[a] All measurements as CH_2Cl_2 solutions. [b] Conditions: CH_2Cl_2; Pt-wire auxiliary, Pt working, and SCE reference electrodes; ferrocene/ferrocenium couple located at 0.46 V [[ΔE(mV) = 80]. [c] RuIII/IV. [d] Thiophene-centered oxidation.

Table 4. Cubic Nonlinear Optical Responses for Complexes 4b−e[a]

compound	C × 10^{-4} (M L^{-1})	α (cm^{-1})	$\chi^{(3)}$ × 10^{20} (m^2/V^2)	$\chi^{(3)}/\alpha$ × 10^{-18} (m^3/V^2)	γ × 10^{44} (m^5/V^2)
4b	2.8	7.8	0.40	5.1	1.5
4c	2.6	5.1	1.20	23	4.9
4d	2.4	12.9	2.10	19	9.1
4e	2.5	13.7	2.50	15	10.4
CS_2	≈ 0	1.94		4.7 × 10^{-5}	

[a] All measurements in THF solutions. α = linear absorption coefficient, $\chi^{(3)}$ = third-order susceptibility, $\chi^{(3)}/\alpha$ = merit factor, γ = second-order hyperpolarizability.

= 1.40 V can only be assigned to the Ru(III/IV) oxidation. In complexes **4b**−**e**,[21] as the potentiel $E_{1/2}$ of this second wave significantly decreases (from 1.35 for **4b** to 0.99 V vs SCE for **4d**) as the length of the π-spacer increases, it was assigned to the oxidation of the thiophene-based spacers by analogy with previous reports on both oligothiophenes[26] and alkynyl-ruthenium derivatives bearing oligothiophene groups.[21]

The extent of the communication between the electron-donating and -accepting termini can be evaluated by comparing the $E_{1/2}$ values of the electrochemically reversible one-electron Ru(II/III) oxidation in complexes **4a**−**e**. The effect of the acceptor on the oxidation of the metal center is highly dependent on the length of the π-bridge (Table 3). In particular, the half-wave potentials ($E_{1/2}$) of the Ru(II/III) oxidation are negatively shifted through insertion of thienyl rings (from **4b** to **4c** or **4d**) or an additional double bond (**4e**). Moreover, the donor effect of the oligothienyl spacers apparently counterbalances the acceptor effect of the formyl end as the separation of the termini increases. For instance, the Ru(II/III) oxidation in complex **4e** becomes close to that of *trans*-[Ru(4-C≡C−C_6H_5)Cl(dppe)$_2$] ($E_{1/2}$ = 0.45 V vs SCE).[27]

Third-Order Nonlinearity Measurements. Third-order nonlinearities for the complexes **4b**−**e** were evaluated by degenerate four-wave mixing measurements (DFWM)[28] at 532 nm in chloroform solutions (0.3 g/L). Details of the measurements and theoretical approach are given in the Supporting Information. We found that the molecules **4a**−**e** exhibit large third-order hyperpolarizability (γ) values (approximately 10^5 times larger than those of CS_2, which is a reference material for DFWM) (Table 4).

Extension of the acetylide ligand from the one-ring spacer in **4b** to the two-ring system **4c** leads to a large increase in γ, which parallels results observed in all-organic chromophores. Not surprisingly, these results are consistent with that of M. G. Humphrey, which demonstrated an electronic origin for cubic nonlinearities in the metal-acetylide complexes.[29] Significant extension of the π-system on proceeding from **4c**, to **4d**, to **4e** results in a further increase in γ. Complex **4e** has the largest γ response for this series of complexes: the present data complement the results obtained for linear absorption, indicating that electronic communication through the dithienylethylene-linked spacer (complex **4e**) is the most efficient in this series.[30] These data also suggest that extending π-delocalization in similar systems must be carried out in order to give a minimal aromatic character on the π-conjugated bridge.

Acoustically Induced Second-Order Nonlinearity Measurements. Incorporating organometallic chromophores within optically transparent and electrically neutral polymers may be considered as a way to achieve promising materials for second-order optical effects.[17] Therefore, we investigated the inclusion of the organometallic complexes **4b**−**e** within polymethylmethacrylate (PMMA) matrixes in order to get processable materials. Samples **S4c**−**e** were prepared by mixing 4 g of PMMA (M_w = 120 000) and 0.035 g of the different complexes **4c**−**e** in solution in chloroform. The inclusion of complexes **4** was obtained by slow evaporation of the solvent. UV−visible measurements on films of these samples deposited on glass ascertained the inclusion of complexes **4** in the PMMA matrixes, as indicated by broad absorptions bands at 500, 510, and 530 nm for **S4c**, **S4d**, and **S4e**, which are close to that observed for the corresponding parent complexes. IR spectra that display characteristic ν(C≡C) (2038−2041 cm^{-1}) and ν(CH=O) (1586−1593 cm^{-1}) absorption bands confirmed their presence. Then, we investigated acoustically induced nonlinear optical properties of these samples. Acoustically induced second-harmonic generation (AISHG) is related with physical effects at the atomic scale that can result from interactions of phonons with the electron subsystem of ionic or polarizable molecules in the solid state. In particular, it was established[31] that electron−hole and electron−phonon interactions could result in a local asymmetry.[32] The resulting spatial non-centrosymmetry would be thus at the origin of the observed NLO responses. Acoustically induced SHG[18,33] was first observed in composites

(26) Jestin, I.; Frère, P.; Blanchard, P.; Roncali, J. *Angew. Chem. Int. Ed.* **1998**, *37*, 942.
(27) McDonagh, A. M.; Cifuentes, M. P.; Humphrey, M. G.; Houbrechts, S.; Persoons, A. *J. Organomet. Chem.* **2000**, *610*, 71.
(28) Sahraoui, B.; Rivoire, G. *Opt. Commun.* **1997**, *138*, 109.
(29) Whittall, I. R.; Humphrey, M. G.; Samoc, M.; Swiatkiewicz, J.; Luther-Davies, B. *Organometallics* **1995**, *14*, 5493.
(30) Roncali, J. *Acc. Chem. Res.* **2000**, *33*, 147.
(31) (a) Bussmann-Holder A.; Buttner, H. *Nature* **1992**, ***360***, 541. (b) Dalal, N.; Klymachyov, A.; Bussmann-Holder, A. *Phys. Rev. Lett.* **1998**, *81*, 5924. (c) Sahraoui, B.; Kityk, I. V.; Nguyen Phu, X.; Hudhomme, P.; Gorgues, A. *Phys. Rev. B* **1999**, *59*, 9229.
(32) Bielincher, V. I.; Sturman, B. I. *Usp. Fiz. Nauk* **1980**, *130*, 415.
(33) Majchrowski, A.; Kityk, I. V.; Kasperczyk, J.; Łukasiewicz, T.; Mefleh, A. *Mater. Lett.* **2001**, *50*, 146.

Table 5. Maximal AIOSHG Values for Complexes 4c−e Included in PMMA Matrixes and for Selected Ferroelectric and Photorefractive Crystals

compound	$\chi^{(2)}$ (pm/V)	T (K)[a]
4c[b]	0.80	4.2
4d[b]	0.27	4.2
4e[b]	0.64	4.2
$Ba_2NaNb_5O_{15}$	0.17	106
$Bi_4Ge_3O_{12}$	0.36	153
$LiNbO_3$	0.12	92
$Pb_3Ge_5O_{12}$	0.61	4.2

[a] Temperature at which the measurement was achieved. [b] 0.035 g of **4** incorporated in 4 g of PMMA.

containing large-size nanocrystallites and in ferroelectric photorefractive crystals.[34]

We investigated AISHG in the σ-acetylide complexes **4c**−**e** incorporated within PMMA matrixes in the form of plates with thickness within 1.4 mm. The experimental setup for the AISHG measurements is fully described in the Supporting Information. The acoustical signal power has been applied to the sample by $LiNbO_3$ piezoelectric acoustical transducers, which allow varying acoustical frequencies (80 Hz to 1.1 MHz). A pulsed mode-locked YAB-Gd^{3+} laser ($\lambda = 1.76$ μm, power about 25 MW; pulse duration about 15 ps) was used as a source of optical second-harmonic generation (fundamental laser beam).

The observed effect was maximal for parallel directions of the acoustical wave polarization and fundamental light beam polarization, with effective second-order susceptibility $\chi^{(2)}$ as high as 0.8 pm/V for **4c** (Table 5). It should also be stressed that when similar experiments were carried out in the absence of acoustic signal, we did not observe any nonlinear response.

The differences in the order for the observed values (**4c** > **4e** > **4d**) and the order for the linear optical and third-order NLO measurements (**4e** > **4d** > **4c**) were unexpected. Actually, the AISHG data seem to be inconsistent with the effect of an extension of the π-conjugation pathway. To better understand these differences, a new set of experiments was performed. We thus observed a substantial influence of the angle Φ between the sample surface and laser beam polarization on the second-order nonlinear optical output signal stimulated by the acoustical field. Thus, the output AISHG intensities increase with increasing the effective thickness of the sample, by rotating it with respect to the light beam propagation. On the other hand, maximal increase was observed at acoustical power densities about 1.2 W/cm^2 with increasing differences for **4e** compared to **4c**,**d**.

Temperature-dependent measurements of the AISHG also show a drastic increase of the output signal at temperatures below 45 K. Such behavior can be associated with the optical SHG temperature dependence during the structural phase transition in disordered material.[35] Moreover, the AISHG signal correlates well with the temperature behavior of differential scanning calorimetry. These experimental data, particularly the nonlinear dependences of the AISHG on acoustical power as well as sensitivity to morphological phase transformation, indicate that the origin of the observed phenomenon results from a spatial non-centrosymmetry induced by phonons interacting with the electron subsystems.[36]

To compare our results with that of typical ferroelectric and photorefractive crystals, similar AISHG measurements were done for several of these crystals. The corresponding maximal second-order susceptibilities $\chi^{(2)}$ were evaluated by varying acoustical strengths at different temperatures (Table 5). The maximal value of the AIOSHG (0.8 pm/V) for complex **4c** incorporated in the PMMA matrixes is then comparable with the values for these nonlinear optical single crystals. We continue this study to determine the factors that could improve the AISHG responses. These results will be published in due course.

Concluding Remarks

The present work reports a high-yield synthetic access to a new series of alkynyl ruthenium donor−π-acceptor complexes bearing oligothiophene-conjugating bridges. Complexes **4a**−**e** present third-NLO activity. The γ maxima follow the same order as the absorption energies. Absorption and third-order nonlinear properties increase by extending the effective conjugation in this series of complexes. In addition, acoustically induced second-harmonic generation has been observed for films of the complexes **4c**−**e** incorporated in PMMA matrixes. The actual AISHG values are comparable with that observed for the well-known ferroelectric and photorefractive crystals. Therefore, these complexes can be considered as attractive candidates for SHG applications and in the perspective of molecular materials for optical communication systems.

Experimental Section

General Information. Reactions were carried out using standard Schlenk techniques, under an inert atmosphere. Solvents were dried and distilled according to standard procedures.[37] The following were prepared by literature procedures: bromodithiophenecarboxaldehyde (**1c**),[38] bromoterthiophenecarboxaldehyde (**1d**),[39] 4-ethynylbenzaldehyde,[39] and *trans*-[RuCl(dppe)$_2$][OTf].[20b] Column chromatography was carried out on Merck silica gel 60 (70−230 ASTM) or Merck alumina oxide 90 active basic (activity grade II, 70−230 mesh ASTM). Microanalyses were carried out at the Center for Microanalyses of the CNRS at Lyon-Solaise, France. Routine NMR spectra were recorded using a Bruker DPX 200 spectrometer. High-field NMR spectra experiments were performed on a multinuclear Bruker WB 300 instrument or a Bruker Avance DRX 500. Chemical shifts are given in parts per million relative to tetramethylsilane (TMS) for ^{1}H and ^{13}C NMR spectra and H_3PO_4 for ^{31}P NMR spectra. Electrochemical data were acquired with a computer-controlled Autolab PG start 30 potentiostat utilizing the GPES program version 4.7.

(34) (a) Majchrowski, A. I.; Kityk, V.; Lukasiewicz, T.; Mefleh, A.; Benet, S. *Opt. Mater.* **2000** *15* (1), 51. (b) Majchrowski, A.; Mefleh, A.; Lee, R.; Makowska-Janusik, M.; Kasperczyk, J.; Kityk, I. V.; Berdowski, J.; Benet, S. *Nonlinear Opt.* **2000**, *24*, 335 (c) Dalal, N.; Klymachyov, A.; Bussmann-Holder, A. *Phys. Rev. Lett.* **1998**, *81*, 5924.
(35) Napieralski, J. *Ferroelectrics* **1999**, *220*, 17.
(36) (a) Majchrowski, A.; Mija, J. *Mater. Sci. Eng. A* **1993**, *173*, 19. (b) Liu, Q.; Zhao, X.; Tanaka, K.; Narazaki, A.; Hirao, K.; Gan, F. *Opt. Commun.* **2001**, *198*, 187.
(37) Leonard, J.; Lygo, B.; Procter, G. *Advanced Practical Organic Chemistry*, 2nd ed.; Blackie Academic & Professional: New York, 1995.
(38) Wei, Y.; Wang, B.; Tian, J. *Tetrahedron Lett.* **1995**, *36*, 665.
(39) Austin, W. B.; Bilow, N.; Kelleghan, W. J.; Lau, K. S. Y. *J. Org. Chem.* **1981**, *46*, 2280.

Electrochemical experiments were performed with 10^{-4} M methylene chloride solution of the complexes in a standard three-electrode system (platinum working/auxiliary electrode and SCE reference electrode). Bu_4NPF_6 [0.1 M] was used as the supporting electrolyte. Scan rates were typically 100 mV s^{-1}. Transmittance-FTIR spectra were recorded using a Bruker IFS 28 spectrometer or a Perkin-Elmer 841 spectrophotometer by using samples embedded in KBr disks or thin films between NaCl plates. UV−vis spectra were recorded on a UVIKON spectrometer. Secondary ion (SI) mass spectra were recorded on a VG ZAB 2SEQ spectrometer (30 kV Cs^+ ions, current 1 mA, accelerating potential 8 kV, matrix *o*-nitrophenyloctyl ether or *m*-nitrobenzylic alcohol) and electron impact (EI), including high-resolution (HR), mass spectra on a VG Autospec instrument (70 eV electron energy, 8 kV accelerating potential) at the Centre de Mesures Physiques de l'Ouest, Rennes, France. Peaks are reported as *m/z* (assignment, relative intensity).

Synthesis of (*E*)-1-(5-Bromo-2-thienyl)-2-(5-formyl-2-thienyl)ethene (1e). A solution of *N*-bromosuccinimide (0.40 g, 2.25 mmol) in DMF (15 mL) was added dropwisely over a period of 45 min to a solution of 5-[(*E*)-2-(2-thienyl)vinyl]-thiophene-2-carbaldehyde[15a] (0.45 g, 2.04 mmol) in DMF (50 mL) cooled to 0 °C under N_2 in the absence of light. The mixture was stirred for 18 h at room temperature and concentrated, and the residue was diluted with CH_2Cl_2 (200 mL). The organic phase was washed with water (2 × 75 mL), dried over $MgSO_4$, and evaporated to dryness. The residue was triturated with pentane, and the mixture was filtered, leading to a yellow-brown solid, which was further purified by chromatography on silica gel (eluent: CH_2Cl_2/cyclohexane, 7:3) to give a yellow powder (0.42 g, 69% yield). An analytical sample was recrystallized from a mixture of CH_2Cl_2 and hexane, affording yellow crystals. Mp: 129−130 °C (lit. 129−131 °C).[19a] ^{1}H NMR ($CDCl_3$, 500.13 MHz, δ ppm): 9.85 (s, 1H, CHO); 7.64 (d, 1H, $^3J_{HH}$ = 3.9 Hz); 7.13 (d, 1H, $^3J_{HH}$ = 15.4 Hz); 7.11 (d, 1H, $^3J_{HH}$ = 3.9 Hz); 6.98 (d, 1H, $^3J_{HH}$ = 3.9 Hz); 6.89 (d, 1H, $^3J_{HH}$ = 15.4 Hz); 6.87 (d, 1H, $^3J_{HH}$ = 3.9 Hz). ^{13}C{^{1}H} NMR ($CDCl_3$, 125.7 MHz, δ ppm): 182.39, 151.37, 142.88, 141.78, 137.05, 130.89, 128.21, 126.74, 124.95, 120.63, 113.26. IR (KBr): $\nu_{C=O}$ 1654 cm^{-1}.

Synthesis of Ligands 2a−e. General Procedure for the Preparation of Trimethylsilyl-Protected Acetylene (2b−e). To a mixture of $PdCl_2(PPh_3)_2$ (175 mg, 0.25 mmol) and CuI (95 mg, 0.5 mmol) in 40 mL of THF were added successively 10 mmol of the corresponding bromo derivatives **1b−e**, 11 mmol of trimethylsilyl acetylene (1.56 mL), and 40 mL of triethylamine.[40] The resulting mixture was stirred for 24 h at room temperature. The dark solution was pumped dry, and the resulting black solid was extracted with pentane (4 × 50 mL) and further purified by chromatography on silica gel (eluent pentane). The resulting solution was dried over $MgSO_4$, filtered, and pumped dry to afford **2b−e** as powdery solids.

5-Trimethylsilylethynylthiophene-2-carbaldehyde (2b). A total of 1.75 g of compound **2b** was obtained as a white-brown solid in 84% yield from 1.91 g of 5-bromothiophene-2-carbaldehyde. ^{1}H NMR ($CDCl_3$, 200 MHz, δ ppm): 9.81 (s, 1H, CHO), 7.59 (d, 1H, $^3J_{HH}$ = 3.9 Hz), 7.24 (d, 1H, $^3J_{HH}$ = 3.9 Hz), 0.23 (s, 9H). ^{13}C{^{1}H} NMR ($CDCl_3$, 50 MHz, δ ppm): 179.20, 142.29, 139.51, 133.13, 123.08, 100.30, 95.13, −0.10; IR (KBr): $\nu_{C\equiv C}$ 2148.9 cm^{-1}, $\nu_{C=O}$ 1673 cm^{-1}. UV/vis (CH_2Cl_2): λ_{max} (ϵ) 328 nm (2600 mol^{-1} L cm^{-1}).

5′-Trimethylsilylethynyl-[2,2′]bithiophene-5-carbaldehyde (2c). From 2.73 g of 5′-bromo-[2,2′]bithiophene-5-carbaldehyde,[39] 2.38 g of compound (**2c**) was obtained as a yellowish solid in 82% yield. ^{1}H NMR ($CDCl_3$, 200 MHz, δ ppm): 9.86 (s, 1H, CHO), 7.65 (d, 1H, $^3J_{HH}$ = 4 Hz), 7.24 (d, 1H, $^3J_{HH}$ = 4 Hz), 7.19 (d, 1H, $^3J_{HH}$ = 4 Hz), 7.15 (d, 1H, $^3J_{HH}$ = 4 Hz), 0.26 (s, 9H). ^{13}C{^{1}H} NMR ($CDCl_3$, 50 MHz, δ ppm): 183.22, 146.82, 142.91, 142.90, 138.11, 137.89, 134.21, 126.40, 125.18, 102.30, 97.23, −0.10; IR (KBr): $\nu_{C\equiv C}$ 2142.6 cm^{-1}, $\nu_{C=O}$ 1636 cm^{-1}. UV/vis (CH_2Cl_2): λ_{max} 378 nm (ϵ 3500 mol^{-1} L cm^{-1}). MS (EI): *m/z* calcd $[M]^+$ = 290.0255; *m/z* found $[M]^+$ = 290.0258.

5″-Trimethylsilylethynyl-[2,2′;5′,2″]terthiophene-5-carbaldehyde (2d). From 3.55 g of 5″-bromo-[2,2′;5′,2″]terthiophene-5-carbaldehyde,[39] 2.61 g of compound (**2d**) was obtained as a yellow-orange solid in 70% yield. ^{1}H NMR ($CDCl_3$, 200 MHz, δ ppm): 9.92 (s, 1H, CHO), 7.74 (d, 1H, $^3J_{HH}$ = 6 Hz), 7.33 (d, 1H, $^3J_{HH}$ = 4 Hz), 7.31 (d, 1H, $^3J_{HH}$ = 4 Hz), 7.21 (d, 1H, $^3J_{HH}$ = 4 Hz), 7.19 (d, 1H, $^3J_{HH}$ = 4 Hz), 7.12 (d, 1H, $^3J_{HH}$ = 4 Hz), 0.32 (s, 9H). ^{13}C{^{1}H} NMR ($CDCl_3$, 50 MHz, δ ppm): 182.64, 146.66, 141.99, 138.44, 137.85, 137.55, 135.31, 133.77, 127.13, 125.34, 124.46, 124.19, 123.04, 101.52, 97.24, 0.10. IR (KBr): $\nu_{C\equiv C}$ 2144 cm^{-1}; $\nu_{C=O}$ 1634 cm^{-1}. MS (EI): *m/z* calcd $[M]^+$ = 372.0132; *m/z* found $[M]^+$ = 372.0142.

(*E*)-1-(5-Trimethylsilylethynyl-2-thienyl)-2-(5-formyl-2-thienyl)ethene (2e).[15f] A total of 2.33 g of compound **2e** was obtained as a yellow solid in 74% yield from 2.99 g of *E*-1-(5-bromo-2-thienyl)-2-(5-formyl-2-thienyl)ethene, **1e**. ^{1}H NMR ($CDCl_3$, 200 MHz, δ ppm): 9.84 (s, 1H), 7.65 (d, 1H, $^3J_{HH}$ = 4 Hz), 7.16 (d, 1H, $^3J_{HH}$ = 15.8 Hz), 7.12 (d, 1H, $^3J_{HH}$ = 4 Hz), 7.11 (d, 1H, $^3J_{HH}$ = 4 Hz), 6.97 (d, 1H, $^3J_{HH}$ = 4 Hz), 6.96 (d, 1H, $^3J_{HH}$ = 15.8 Hz), 0.31 (s, 9H). ^{13}C{^{1}H} NMR ($CDCl_3$, 50 MHz, δ ppm): 182.96, 151.89, 143.01, 142.15, 137.69, 133.99, 128.36, 127.43, 125.55, 123.94, 121.52, 101.76, 97.89, 0.26. IR (KBr): $\nu_{C\equiv C}$ 2146 cm^{-1}; $\nu_{C=O}$ 1632 cm^{-1}. MS (EI): *m/z* calcd $[M]^+$ = 316.0412; *m/z* found $[M]^+$ = 316.0400.

General Procedure for the Preparation of 3b−e. To a stirred solution of 5 mmol of the trimethylsilyl-protected acetylene derivatives **2b−e** in 30 mL of THF was added 7.5 mmol of Bu_4NF (solution 1 M/THF, 7.5 mL). The mixture was stirred for 1 h at room temperature and concentrated, and the residue was diluted with diethyl ether (3 × 50 mL) and washed with water (3 × 30 mL). The organic phase was dried over $MgSO_4$, filtered, and pumped dry. The resulting organic compound was dissolved in 5 mL of diethyl ether and filtered through a silica gel column with diethyl ether to afford **3b−e** in good yields.

5-Ethynylthiophene-2-carbaldehyde (3b).[15f] From 1.04 g of 5-trimethylsilylethynylthiophene-2-carbaldehyde, **2b**, 572 mg of **3b** was obtained as a brown solid in 84% yield. ^{1}H NMR ($CDCl_3$, 200 MHz, δ ppm): 9.86 (s, 1H), 7.63 (d, 1H, $^3J_{HH}$ = 4 Hz), 7.31 (d, 1H, $^3J_{HH}$ = 4 Hz), 3.57 (s, 1H). ^{13}C{^{1}H} NMR ($CDCl_3$, 50 MHz, δ ppm): 180.20, 142.89, 139.41, 135.69, 122.30, 84.52, 77.40. IR (KBr): $\nu_{C\equiv C}$ 2140 cm^{-1}; $\nu_{C=O}$ 1634 cm^{-1}. MS (EI): *m/z* calcd $[M]^+$ = 135.9983; *m/z* found $[M]^+$ = 135.9999

5′-Ethynyl-[2,2′]bithiophene-5-carbaldehyde (3c).[15f] From 1.45 g of 5′-trimethylsilylethynyl-[2,2′]bithiophene-5-carbaldehyde, **2c**, 972 mg of compound **3c** was obtained as a brownish solid in 89% yield. ^{1}H NMR ($CDCl_3$, 200 MHz, δ ppm): 9.93 (s, 1H), 7.74 (d, 1H, $^3J_{HH}$ = 4 Hz), 7.25 (d, 1H, $^3J_{HH}$ = 4 Hz), 7.21 (s, 2H), 3.53 (s, 1H). ^{13}C{^{1}H} NMR ($CDCl_3$, 50 MHz, δ ppm): 182.99, 146.24, 142.73, 137.85, 137.66, 134.63, 126.12, 125.29, 123.87, 84.06, 76.74. IR (KBr): $\nu_{C\equiv C}$ 2143 cm^{-1}; $\nu_{C=O}$ 1630 cm^{-1}. MS (EI): *m/z* calcd $[M]^+$ = 217.9860; *m/z* found $[M]^+$ = 217.9871.

5″-Ethynyl-[2,2′;5′,2″]terthiophene-5-carbaldehyde (3d). From 1.86 g of 5″-trimethylsilylethynyl-[2,2′;5′,2″]terthiophene-5-carbaldehyde, **3d**, 976 mg of compound **3d** was obtained as a yellowish solid in 65% yield. ^{1}H NMR ($CDCl_3$, 200 MHz, δ ppm): 9.93 (s, 1H), 7.74 (d, 1H, $^3J_{HH}$ = 6 Hz), 7.34 (d, 1H,

(40) (a) Kim, J. P.; Masai, H.; Sonogashira, K.; Hagihara, N. *Inorg. Nucl. Chem. Lett.* **1970**, *6*, 181. (b) Sonogashira, K.; Yatake, T.; Tohda, Y.; Takahashi, S.; Hagihara, N. *J. Chem. Soc., Chem. Commun.* **1977**, 291. (c) Sonogashira, K.; Fujikura, Y.; Yatake, T.; Takahashi, S.; Hagihara, N. *J. Organomet. Chem.* **1978**, *145*, 101.

$^3J_{HH}$ = 4 Hz), 7.32 (d, 1H, $^3J_{HH}$ = 4 Hz), 7.22 (d, 1 H, $^3J_{HH}$ = 4 Hz), 7.21 (d, 1 H, $^3J_{HH}$ = 4 Hz), 7.14 (d, 1 H, $^3J_{HH}$ = 4 Hz), 3.50 (s, 1 H). $^{13}C\{^1H\}$ NMR ($CDCl_3$, 50 MHz, δ ppm): 182.90, 146.85, 138.45, 137.77, 135.74, 134.51, 132.41, 127.95, 127.37, 125.76, 124.76, 124.40, 122.58, 83.33, 76.49. IR (KBr): $\nu_{C\equiv C}$ 2144 cm^{-1}; $\nu_{C=O}$ 1628 cm^{-1}. MS (EI): *m/z* calcd $[M]^+$ = 299.9737; *m/z* found $[M]^+$ = 299.9729.

5-[2-(5-Ethynylthiophen-2-yl)vinyl]thiophene-2-carbaldehyde (3e).[15f] From 1.58 g of 5-[2-(5-trimethylsilylethynylthiophen-2-yl)vinyl]thiophene-2-carbaldehyde (**2e**), 978 mg of compound (**3e**) was obtained as a deep yellow solid in 80% yield. ^1H NMR ($CDCl_3$, 200 MHz, δ ppm): 9.85 (s, 1H), 7.65 (d, 1 H, $^3J_{HH}$ = 4 Hz), 7.18 (d, 1 H, $^3J_{HH}$ = 15.8 Hz), 7.17 (d, 1H, $^3J_{HH}$ = 4 Hz), 7.13 (d, 1 H, $^3J_{HH}$ = 4 Hz), 6.99 (d, 1H, $^3J_{HH}$ = 4 Hz), 6.98 (d, 1H, $^3J_{HH}$ = 15.8 Hz), 3.45 (s, 1H). $^{13}C\{^1H\}$ NMR ($CDCl_3$, 50 MHz, δ ppm): 182.99, 151.75, 143.34, 142.27, 137.67, 134.42, 128.21, 127.53, 125.39, 122.67, 121.81, 83.63, 77.68. IR (KBr): $\nu_{C\equiv C}$ 2143 cm^{-1}; $\nu_{C=O}$ 1631 cm^{-1}. MS (EI): *m/z* calcd $[M]^+$ = 244.0016; *m/z* found $[M]^+$ = 244.0007.

Synthesis of Complexes 4a−e. General Procedure. To a mixture of [*cis*-(Cl)(dppe)$_2$Ru][TfO][20b] (542 mg, 0.5 mmol) and **3a−e** (0.6 mmol) was added 50 mL of dichloromethane. The resulting mixture was stirred at room temperature for 20 h, and the solvant was pumped dry. The resulting solid was cleaned with diethyl ether (3 × 20 mL) to eliminate the organic reactant. The solid was dissolved in 20 mL of dichloromethane, and 140 μL of NEt_3 (101 mg, 1 mmol) was added, with rapid stirring, at room temperature for 1 h. The resulting solution was washed with water (2 × 50 mL), dried over $MgSO_4$, filtered, and pumped dry. The resulting organometallic compound was dissolved in 5 mL of dichloromethane and filtered through a silica gel column with diethyl ether. Finally, solvent was pumped dry to afford powdery solid **4a−e** in 74−95% yields. Analytical samples of **4c−e** were recrystallized from mixtures of CH_2Cl_2 and hexane, affording brown to red crystals.

***trans*-[Ru(4-C≡CC$_6$H$_4$CHO)Cl(dppe)$_2$] (4a).**[25] From 78 mg of acetylene derivative **2a** and 542 mg of [*cis*-(Cl)(dppe)$_2$Ru][TfO], 504 mg of compound **4a** was obtained as a yellow powdery solid in 95% yield. ^1H NMR ($CDCl_3$, 300 MHz, δ ppm): 9.79 (s, 1H, CHO), 7.51 (d, 2H, $^3J_{HH}$ = 5.5 Hz), 7.19−6.86 (m, 40H, dppe), 6.51 (d, 2H, $^3J_{HH}$ = 5.5 Hz), 2.61 (m, 8H, CH_2 dppe). $^{13}C\{^1H\}$ NMR ($CDCl_3$, 75 MHz, δ ppm): 191.44 (CHO), 142.5 (quint., Ru−C≡C, $^2J_{PC}$ = 15.8 Hz), 136.79 (C_{quat}, C_6H_4), 136.01 (quint., C_{ipso}, $|^1J_{PC} + {}^3J_{PC}|$ = 12 Hz, dppe phenyl groups), 135.41 (quint., C_{ipso}, $|^1J_{PC} + {}^3J_{PC}|$ = 12 Hz, dppe phenyl groups), 134.40 and 134.09 (CH, dppe phenyl groups), 130.82 (C_{quat}, phenyl), 130.24, 129.43, 129.01, 127.33, and 127.08 (CH, dppe phenyl groups), 115.81 (Ru−C≡C), 30.86 (quint., PCH_2-CH_2P, $|^1J_{PC} + {}^3J_{PC}|$ = 23 Hz). $^{31}P\{^1H\}$ NMR ($CDCl_3$, 121 MHz, δ ppm): 49.50 (s, dppe). IR (KBr): $\nu_{C\equiv C}$ 2036 cm^{-1}; $\nu_{C=O}$ 1584 cm^{-1}. UV/vis (CH_2Cl_2): λ_{max} (ϵ) 258 nm (19 000 mol^{-1} L cm^{-1}), 423 nm (12r t900 mol^{-1} L cm^{-1}). MS (LSIMS): *m/z* calcd $[M]^+$ = 1062.1779; *m/z* found $[M]^+$ = 1062.1768

***trans*-[Ru(2,5-C≡CC-th-CHO)Cl(dppe)$_2$] (4b).** From 82 mg of reactant **2b** and 542 mg of [*cis*-(Cl)(dppe)$_2$Ru][TfO], 454 mg of compound **4b** was obtained as a brownish powdery solid in 85% yield. ^1H NMR ($CDCl_3$, 300 MHz, δ ppm): 9.63 (s, 1H, CHO), 7.47 (d, 1H, $^3J_{HH}$ = 4.0 Hz), 7.44−6.96 (m, 40H, dppe), 5.99 (d, 1H, $^3J_{HH}$ = 4.0 Hz), 2.65 (m, 8H). $^{13}C\{^1H\}$ NMR ($CDCl_3$, 50 MHz, δ ppm): 181.29 (CHO), 154.47 (quint., Ru−*C*≡C, $^2J_{PC}$ = 15.9 Hz), 141.80 and 138.29 (C_{quat}, thiophene), 135.97 (CH, thiophene), 135.56 and 135.19 (quint., C_{ipso}, $|^1J_{PC} + {}^3J_{PC}|$ = 12 Hz, dppe phenyl groups), 134.48, 133.82, 129.14, 127.52, and 127.15 (CH, dppe phenyl groups), 126.60 (s, CH, thiophene), 108.52 (s, Ru−C≡*C*), 30.56 (quint., PCH_2CH_2P, $|^1J_{PC} + {}^3J_{PC}|$ = 23 Hz). $^{31}P\{^1H\}$ NMR ($CDCl_3$, 121 MHz, δ ppm): 49.12 (s, dppe). IR (KBr): $\nu_{C\equiv C}$ 2032 cm^{-1}; $\nu_{C=O}$ 1589 cm^{-1}. UV/vis (CH_2Cl_2): λ_{max} (ϵ) 249 nm (49 000 mol^{-1} L cm^{-1}), 450 nm (27 400 mol^{-1} L cm^{-1}). MS (LSIMS): *m/z* calcd $[M]^+$ = 1068.1343; *m/z* found $[M]^+$ = 1068.1351.

***trans*-[Ru(2,2′,5,5′-C≡C-th-th-CHO)Cl(dppe)$_2$] (4c).** From 130 mg of **2c** and 542 mg of [*cis*-(Cl)(dppe)$_2$Ru][TfO], 466 mg of compound **4c** was obtained as a red-brownish powdery solid in 81% yield. ^1H NMR ($CDCl_3$, 300 MHz, δ ppm): 9.87 (s, 1H), 7.69 (d, 1H, $^3J_{HH}$ = 4.0 Hz), 7.42−7.03 (m, 42H, dppe and th. groups), 6.05 (d, 1H, $^3J_{HH}$ = 4.0 Hz), 2.73 (m, 8H, CH_2 dppe). $^{13}C\{^1H\}$ NMR ($CDCl_3$, 75 MHz, δ ppm): 182.26 (CHO), 141.52 (quint., Ru−*C*≡C, $^2J_{PC}$ = 15.9 Hz), 143.88 and 148.73 (C_{quat}, thiophene), 139.60 and 137.90 (CH, thiophene), 136.10 and 135.95 (quint., C_{ipso}, $|^1J_{PC} + {}^3J_{PC}|$ = 12 Hz, dppe phenyl groups), 134.49, 133.93, 128.99, 127.43, and 127.10 (CH, dppe phenyl groups), 130.51 and 128.51 (C_{quat}, thiophene), 126.45 and 122.01 (CH, thiophene), 106.98 (s, Ru−C≡*C*), 30.61 (quint., PCH_2CH_2P, $|^1J_{PC} + {}^3J_{PC}|$ = 23 Hz). $^{31}P\{^1H\}$ NMR ($CDCl_3$, 121 MHz, δ ppm): 50.01 (s, dppe). IR (KBr): $\nu_{C\equiv C}$ 2042 cm^{-1}; $\nu_{C=O}$ 1587 cm^{-1}. UV/vis (CH_2Cl_2): λ_{max} (ϵ) 270.5 nm (12 500 mol^{-1} L cm^{-1}), 502.5 nm (16 500 mol^{-1} L cm^{-1}). MS (LSIMS): *m/z* calcd $[M]^+$ = 1150.1220; *m/z* found $[M]^+$ = 1150.1203. Anal. Calcd for $C_{63}H_{53}P_4RuClS_2O$: C 65.76; H 4.64. Found: C 65.38; H 4.82.

***trans*-[Ru(−C≡C-th-th-th-CHO)Cl(dppe)$_2$] (4d).** From 180 mg of **2d** and 542 mg of [*cis*-(Cl)(dppe)$_2$Ru][TfO], 480 mg of **4d** was obtained as a red powdery solid in 78% yield. ^1H NMR ($CDCl_3$, 300 MHz, δ ppm): 9.91 (s, 1H), 7.94 (d, 1H, $^3J_{HH}$ = 4.0 Hz), 7.84 (d, 1H, $^3J_{HH}$ = 4.0 Hz, CH thiophene), 7.73 (d, 1H, $^3J_{HH}$ = 4.0 Hz, CH thiophene), 7.48−7.02 (m, 42H, dppe and th. groups), 6.13 (d, 1H, $^3J_{HH}$ = 4.0 Hz), 2.74 (m, 8H, CH_2 dppe). $^{13}C\{^1H\}$ NMR ($CDCl_3$, 75 MHz, δ ppm): 182.39 (CHO), 142.85 (quint., Ru−*C*≡C, $^2J_{PC}$ = 15.9 Hz), 147.48 and 140.75 (C_{quat}, thiophene), 141.00 and 137.33 (CH, thiophene), 136.02 and 135.49 (quint., C_{ipso}, $|^1J_{PC} + {}^3J_{PC}|$ = 12 Hz, dppe phenyl groups), 134.48 and 134.01 (CH, dppe phenyl groups), 133.80, 132.58, 132.13, and 128.94 (C_{quat}, thiophene), 128.95, 127.41, and 127.07 (CH, dppe phenyl groups), 126.04, 124.81, 123.78, and 122.70 (CH, thiophene), 106.83 (s, Ru−C≡*C*), 30.61 (quint., PCH_2CH_2P, $|^1J_{PC} + {}^3J_{PC}|$ = 23 Hz. $^{31}P\{^1H\}$ NMR ($CDCl_3$, 121 MHz, δ ppm): 50.17 (s, dppe). IR (KBr): $\nu_{C\equiv C}$ 2042 cm^{-1}; $\nu_{C=O}$ 1590 cm^{-1}. UV/vis (CH_2Cl_2): λ_{max} (ϵ) 248 nm (60 500 mol^{-1} L cm^{-1}), 510 nm (32 100 mol^{-1} L cm^{-1}). MS (LSIMS): *m/z* calcd $[M]^+$ = 1232.1098; *m/z* found $[M]^+$ = 1232.1108. Anal. Calcd for $C_{67}H_{55}P_4RuClS_3O$: C 63.64; H 4.56. Found: C 63.68; H 4.69.

***trans*-[Ru(−C≡C-th-(*E*)CH=CH-th-CHO)Cl(dppe)$_2$] (4e).** From 146.6 mg of **2e** and 542 mg of [*cis*-(Cl)(dppe)$_2$Ru][TfO], 482 mg of compound **4e** was obtained as a deep red powdery solid in 82% yield. ^1H NMR ($CDCl_3$, 300 MHz, δ ppm): 9.81 (s, 1H), 7.63 (d, 1H, $^3J_{HH}$ = 4 Hz), 7.37−6.98 (m, 42H), 6.87 (d, 1H, $^3J_{HH}$ = 4 Hz, CH thiophene), 6.77 (d, 1H, $^3J_{HH}$ = 16 Hz, =CH), 2.58 (m, 8H, CH_2 dppe). $^{13}C\{^1H\}$ NMR ($CDCl_3$, 75 MHz, δ ppm): 182.30 (CHO), 153.66 (CH=), 143.29 (quint., Ru−*C*≡C, $^2J_{PC}$ = 15.9 Hz), 140.19 and 137.74 (C_{quat} thiophene), 136.04 and 135.32 (quint., C_{ipso}, $|^1J_{PC} + {}^3J_{PC}|$ = 12 Hz, dppe phenyl groups), 134.61 (=CH), 134.49 and 134.02 (CH, dppe phenyl groups), 133.18 (C_{quat}, thiophene), 129.66 (CH, thiophene), 129.07, 129.02, 127.44, and 127.12 (CH, dppe phenyl groups), 127.00, 125.28, and 116.57 (CH, thiophene), 108.21 (Ru−C≡*C*), 30.67 (quint., PCH_2CH_2P, $|^1J_{PC} + {}^3J_{PC}|$ = 23 Hz). $^{31}P\{^1H\}$ NMR ($CDCl_3$, 121 MHz, δ ppm): 49.44 (s, dppe). IR (KBr): $\nu_{C\equiv C}$ 2038 cm^{-1}; $\nu_{C=O}$ 1593 cm^{-1}. UV/vis (CH_2Cl_2): λ_{max} (ϵ) 254 nm (82 000 mol^{-1} L cm^{-1}), 528 nm (55 500 mol^{-1} L cm^{-1}). MS (LSIMS): *m/z* calcd $[M]^+$ = 1176.1377; *m/z* found $[M]^+$ = 1176.1391. Anal. Calcd for $C_{65}H_{55}P_4RuClS_2O{\cdot}2CH_2Cl_2$ (consistent with the NMR spectra and X-ray structure determination): C 59.76; H 4.42. Found: C 59.49; H 4.42.

X-ray Structure Determinations of 1e and 4e. Single crystals of **1e**, suitable for X-ray crystallographic analysis, were obtained from a methylene chloride/hexane solution. Data collection was performed at 294 K on an Enraf-Nonius MACH3 four-circle diffractometer equipped with a graphite monochromator utilizing Mo Kα radiation (λ = 0.71073 Å). The structure

was solved by direct methods (SIR)[41] and refined on F by full matrix least-squares techniques using MolEN package programs.[42] All non-H atoms were refined anisotropically. Absorption was corrected by psi-scan technique, and the H atoms were included in the calculation without refinement.

Crystal data for 1e: $C_{11}H_7Br_1O_1S_2$, $M = 299.21$, orange prism, $0.91 \times 0.74 \times 0.29$ mm^3, monoclinic, $P2_1/c$, $a = 8.0389(7)$ Å, $b = 7.536(1)$ Å, $c = 18.853(2)$ Å, $\beta = 94.48(1)°$, $V = 1138.6(4)$ Å^3, $Z = 4$, $T = 294$ K, $D_{calc} = 1.74$ g/cm^3, GOF = 2.084, $R = 0.054$ [$I > 3\sigma(I)$], $R = 0.096$ (all data).

Single crystals of **4e**, suitable for X-ray crystallographic analysis, were obtained from a methylene chloride/hexane biphasic system. Single crystals were mounted on a Nonius four-circle diffractometer equipped with a CCD camera and a graphite-monochromated Mo Kα radiation source ($\lambda = 0.71073$ Å). Data collection was performed at room temperature. Effective absorption correction was performed (SCALEPACK).[43] Structures were solved with SHELXS-97[44] and refined with SHELXL-97[44] programs by full matrix least-squares method on F^2.

Crystal data for 4e: $C_{67}H_{59}OCl_5P_4RuS_2$; $M = 1346.46$, triclinic, $P\bar{1}$, $a = 9.3070(1)$ Å, $b = 12.9700(2)$ Å, $c = 26.5840(5)$ Å, $\alpha = 84.1060(10)°$, $\beta = 83.0280(10)°$, $\gamma = 80.7530(10)°$, $V = 3132.53(8)$ Å^3, $Z = 2$, $D_{calc} = 1.428$ g cm^{-3}, $T = 293$ K, GOF = 1.029, R1 = 0.0562 [8678 reflns with $I > 2\sigma(I)$], R1 = 0.1122 (14 303 unique data).

Preparation of the Samples S4c−e. Samples **S4c−e** were prepared by mixing the solution of 4 g of PMMA (M_w = 120 000) in 300 mL of $CHCl_3$ and 0.035 g of the different complexes **4b**,**c**,**e** in solution in chloroform (50 mL). The inclusion of the complexes **4** was obtained by slow evaporation of the solvent under a nitrogen flux. They were then obtained in the form of plates with thickness within 1.4 mm by using spin-coating techniques.

S4c: IR (KBr): $\nu_{C\equiv C}$ 2040 cm^{-1}; $\nu_{C=O}$ 1586 cm^{-1}. UV/vis: λ_{max} (ϵ) 503 nm. **S4d**: IR (KBr): $\nu_{C\equiv C}$ 2042 cm^{-1}; $\nu_{C=O}$ 1590 cm^{-1}. UV/vis: λ_{max} (ϵ) 510 nm. **S4e**: IR (KBr): $\nu_{C\equiv C}$ 2040 cm^{-1}; $\nu_{C=O}$ 1593 cm^{-1}. UV/vis: λ_{max} (ϵ) 530 nm.

Supporting Information Available: Full details including txt files of the crystallographic studies of compounds **1e** and **4e**. Text giving experimental procedures for DFWM and AIOSHG measurements. This material is available free of charge via the Internet at http://pubs.acs.org.

OM049236S

(41) SIR92-A program for crystal structure solution. Altomare, A.; Cascarano, G.; Giacovazzo, C.; Guagliardi, A. *J. Appl. Crystallogr.* **1993**, *26*, 343.

(42) *Crystal Structure Analysis*; Molecular Enraf-Nonius (MolEN): Delft Instruments X-ray Diffraction, B. V. Rontnenweg 1 2624 BD Delft, The Netherlands, 1990.

(43) Otwinowski, Z.; Minor, W. Processing of X-ray Diffraction Data Collected in Oscillation Mode. *Methods in Enzymology*, *Macromolecular Crystallography*, *part A*; Carter, C. W., Sweet, R. M., Eds.; Academic Press: New York, 1997; pp 276, 307.

(44) Sheldrick, G. M. *SHELX97*, Program for the Refinement of Crystal Structures; University of Göttingen: Germany, 1997.